Image Synthesis From Reconfigurable Layout and Style

Wei Sun and Tianfu Wu

Department of ECE and the Visual Narrative Initiative, North Carolina State University

{wsun12, tianfu_wu} @ncsu.edu

Abstract

Despite remarkable recent progress on both unconditional and conditional image synthesis, it remains a long-standing problem to learn generative models that are capable of synthesizing realistic and sharp images from reconfigurable spatial layout (i.e., bounding boxes + class labels in an image lattice) and style (i.e., structural and appearance variations encoded by latent vectors), especially at high resolution. By reconfigurable, it means that a model can preserve the intrinsic one-to-many mapping from a given layout to multiple plausible images with different styles, and is adaptive with respect to perturbations of a layout and style latent code. In this paper, we present a layout- and style-based architecture for generative adversarial networks (termed LostGANs) that can be trained end-to-end to generate images from reconfigurable layout and style. Inspired by the vanilla StyleGAN, the proposed LostGAN consists of two new components: (i) learning fine-grained mask maps in a weakly-supervised manner to bridge the gap between layouts and images, and (ii) learning object instance-specific layout-aware feature normalization (ISLA-Norm) in the generator to realize multi-object style generation. In experiments, the proposed method is tested on the COCO-Stuff dataset and the Visual Genome dataset with state-of-the-art performance obtained. The code and pretrained models are available at https://github.com/iVMCL/LostGANs.

1. Introduction

1.1. Motivation and Objective

Remarkable recent progress has been made on both unconditional and conditional image synthesis [6, 27, 35, 23, 1, 24, 17, 18]. The former aims to generate high-fidelity images from some random latent codes. The latter needs to do so with given conditions satisfied in terms of some consistency metrics. The conditions may take many forms such as categorical labels, desired attributes, descriptive sentences, scene graphs, and paired or unpaired images/semantic maps. From the perspective of generative
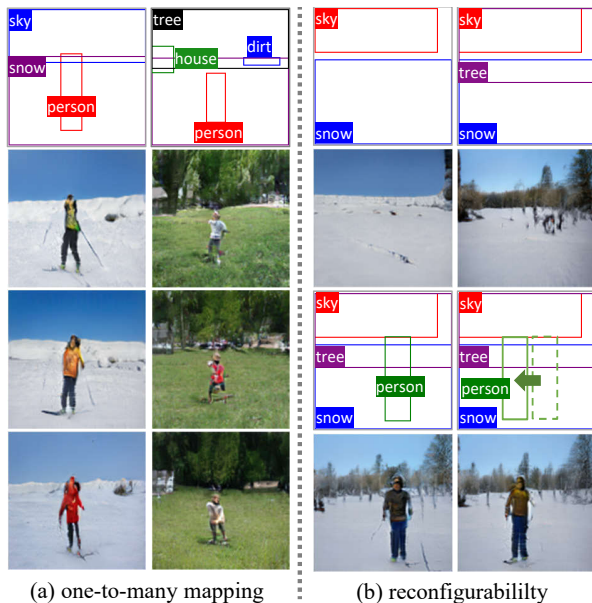

(a) one-to-many mapping   (b) reconfigurabililty

Figure 1. Illustration of the proposed method. *Left:* Our model preserves one-to-many mapping for image synthesis from layout and style. Three samples are generated for each input layout by sampling the style latent codes. *Right:* Our model is also adaptive w.r.t. reconfigurations of layouts (by adding new object bounding boxes or changing the location of a bounding box). The results are generated at resolution 128×128. See text for details.

learning, the solution space of the latter is much difficult to capture than that of the former. Conditional image synthesis, especially with coarse yet complicated and reconfigurable conditions, remains a long-standing problem. Once powerful systems are developed, they can facilitate to pave a way for computers to truly understand visual patterns via analysis-by-synthesis. They will also enable a wide range of practical applications, e.g., generating high-fidelity data for long-tail scenarios in different vision tasks such as autonomous driving.

In this paper, we are interested in conditional image synthesis from layout and style. The layout consists of labeled bounding boxes configured in an image lattice (e.g., 64×64 or 128×128). The style is represented by some latent code. Layout represents a sweet yet challenging spot for
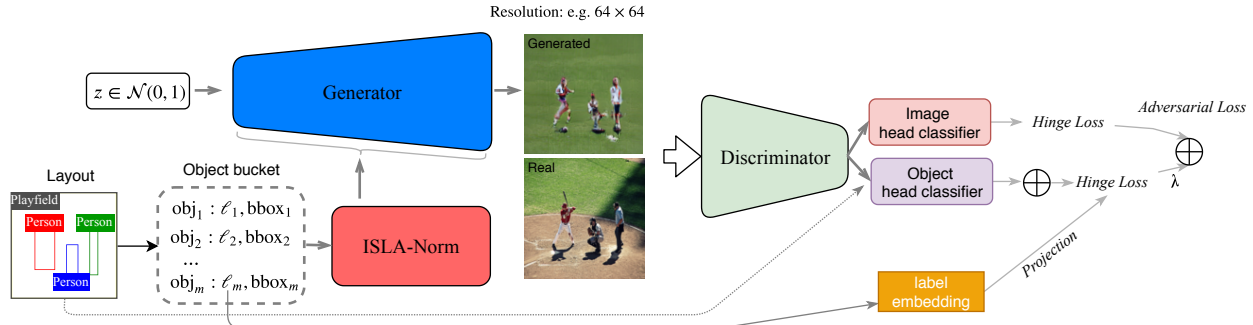
Figure 2. Illustration of the proposed layout- and style-based GANs (LostGANs) for image synthesis from reconfigurable layout and style. Both the generator and discriminator use ResNets as backbones. See text for details.
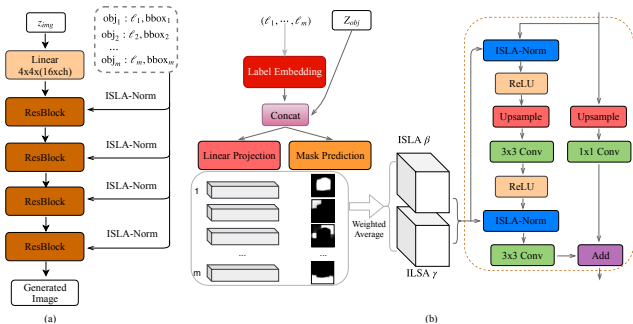

Figure 3. Illustration of the generator (a) and the ISLA-Norm (b) in our LostGAN. See text for details. Best viewed in magnification.

conditional image synthesis: First, layout is usually used as the intermediate representation for other conditional image synthesis such as text-to-image [36, 34] and scene-graph-to-image [16]. Second, layout is more flexible, less constrained and easier to collect than semantic segmentation maps [15, 33]. Third, layout-to-image requires addressing challenging one-to-many mapping and consistent multi-object generation (e.g., occlusion handling for overlapped bounding boxes and uneven, especially long-tail distributions of objects).

Layout-to-image is a relatively new task with many new technical challenges for state-of-the-art image synthesis frameworks and only a few work have been proposed in the very recent literature [16, 12, 38]. Recently, we have seen remarkable progress on the high-fidelity class-conditional image synthesis in ImageNet by the BigGAN [1], and on the amazing style control for specific objects (e.g., faces and cars) by the unconditional StyleGAN [18] (which may be considered as implicitly conditional image synthesis since only one category is usually handled in training). Despite the big successes in generative learning, the problem considered in this paper is still more challenging since the solution space is much more difficult to capture and has much more complicated distributions. For example, we can use the BigGAN to generate a cat image, and as long as the generated image looks realistic and sharp, we think it does a great job. Similarly, we can use the StyleGAN to generate

a face image, and we are happy (even shocked sometimes) if a realistic and sharp face image is generated with a natural style (e.g., smile or sad). Layout-to-image needs to tackle many spatial and semantic (combinatorial) relationships among multiple objects besides the naturalness.

In this paper, we further focus on image synthesis from *reconfigurable* layout and style. By reconfigurable, it means that a model can preserve the intrinsic one-to-many mapping from a given layout to multiple plausible images with different styles, and is adaptive with respect to perturbations of layout and style latent code (Figure 1). State-of-the-art methods on reconfigurable layout-to-image still mainly focus on low resolution (64×64) [16, 38] (which are, in part, due to computationally expensive designs in the pipelines such as convolutional LSTM used in [38]). Beside the resolution issue, another drawback of existing methods is that the diversity of generated images (i.e., style control) is not sufficiently high to preserve the intrinsic one-to-many mapping. We aim to improve both the resolution and the style diversity in reconfigurable layout-to-image.

1.2. Method Overview

To address the challenges in layout-to-image and inspired by the recent StyleGANs [18], we present a **L**ay**O**ut- and **ST**yle-based architecture for GANs (termed *LostGANs*) in the paper (Figure 2).

First, since layout-to-image entails highly expressive neural architectures handling multi-object generation and their diverse occurrence and configurations in layouts. We utilize ResNet [8] for both the generator and discriminator in the proposed LostGAN, as done in the projection-based cGAN [24] and BigGAN [1].

Second, to account for the gap between bounding boxes in a layout and underlying object shapes, we introduce an encoder for layout to predict masks for each bounding box. As we will show in experiments, our LostGAN can predict reasonably good masks in a weakly-supervised manner. The masks help place objects in the generated images with fine-grained geometric properties. So, **we address layout-to-image by computing layout-to-mask-to-**

image (Figure 3), which is motivated by impressive recent progress on conditional image synthesis from semantic label maps [15, 33].

Third, to achieve instance-sensitive and layout-aware style control, we extend the Adaptive Instance Normalization (AdaIN) used in the StyleGAN [18] to **object instance-specific and layout-aware feature normalization (ISLA-Norm)** for the generator for fine-grained spatially distributed multi-object style control. ISLA-Norm computes the mean and variance as done in BatchNorm [14], but computes object instance-specific and layout-aware affine transformations (i.e., gamma and beta parameters) separately for each sample in a min-batch as done in AdaIN (Figure 3). We utilize the projection-based approach proposed in [1]. From the layout encoder, we compute object instance-specific style latent codes (gamma and beta parameters) via simple linear projection. Then, we place the projection-based latent codes in the corresponding predicted masks, and thus induce layout-aware affine transformations for recalibrating normalized feature responses.

Lastly, we utilize both image and object adversarial hinge losses [32, 22] as adopted in [23, 24] in the end-to-end training. Object adversarial loss follows the projection based method in [24] which is the state-of-the-art approach for embedding labels.

We deliberately try to keep our LostGAN as simple as possible by exploiting the best practices in the literature of conditional image synthesis. We hope it can stimulate more exploration on this relatively new task, image synthesis from reconfigurable layout and style.

In experiments, our LostGAN is tested in the COCO-Stuff dataset [2] and the Visual Genome (VG) dataset [20]. It obtains state-of-the-art performance on both datasets in terms of the inception score [30], Frèchet Inception Distance [9], diversity score [37], and classification accuracy [28], which supports the effectiveness of our ILSA-Norm and LostGAN.

2. Related Works

Conditional Image Synthesis. Generative Adversarial Networks (GANs) [6] have achieved great success in image synthesis conditioned on additional input information (i.e. class information [25, 24, 35], source image [19, 39, 13], text description [29, 36], etc). How to feed conditional information to model has been studied in various ways. In [25, 29] vector encoded from conditional information concatenated with noise vector is passed as input to generator. In [3, 5, 1, 26], conditional information is provided to generator by conditional gains and bias in BatchNorm [14] layers. Concurrent work [26] learns spatially adaptive normalization from well annotated semantic masks, while our proposed ISLA-Norm learns from coarse layout information. [29, 4, 36] feed the conditional information into

discriminator by naively concatenation with the input or intermediate feature vector. In [24], projection based way to incorporate conditional information to discriminator effectively improve the quality of class conditional image generation. In our proposed method, layout condition is adopted to generator with ISLA-Norm, and objects information is utilized in projection based discriminator as [24].

Image Synthesis from Layout. Spatial layout conditioned image generation has been studied in recent literature. In [16, 12, 11, 21], layout and object information is utilized in text-to-image generation. [11] controls location of multiple objects in text-to-image generation by adding an object pathway to both the generator and discriminator. [16, 12, 21] performs text-to-image synthesis in two steps: semantic layout (class label and bounding boxes) generation from text first, and image synthesis conditioned on predicted semantic layout and text description. However, [12, 21] requires pixel-level instance segmentation annotation, which is labor intensive to collect, for training of shape generator, while our method does not require pixel-level annotation and can learn segmentation mask in a weakly-supervised manner. [38] studied similar task with us, where variational autoencoders based network is adopted for scene image generation from layout.

Our Contributions. This paper makes the following main contributions to the field of conditional image synthesis.

- It presents a layout- and style-based architecture for GANs (termed LostGANs) which integrates the best practices in conditional and unconditional GANs for a relatively new task, image synthesis from reconfigurable layout and style.

- It presents an object instance-specific and layout-aware feature normalization scheme (termed ISLA-Norm) which is inspired by the projection-based conditional BatchNorm used in cGANs [1] and the Adaptive Instance Normalization (AdaIN) used in StyleGAN [18]. It explicitly accounts for the layout information in the affine transformations.

- It shows state-of-the-art performance in terms of the inception score [30], Frèchet Inception Distance [9], diversity score [37] and classification accuracy [28] on two widely used datasets, the COCO-Stuff [2] and the Visual Genome [20].

3. The Proposed Method

In this section, we first define the problem and then present details of our LostGAN and ISLA-Norm.

3.1. Problem Formulation

Denote by Λ an image lattice (e.g., 64×64). Let $L = \{(\ell_i, bbox_i)_{i=1}^m\}$ be a layout consisting of n labeled bounding boxes, where label $\ell_i \in \mathcal{C}$ (e.g., $|\mathcal{C}| = 171$ in

the COCO-Stuff dataset), and bounding box $bbox_i \subseteq \Lambda$. Different bounding boxes may have occlusions. Let z_{img} be the latent code controlling image style and z_{obj_i} the latent code controlling object instance style for $(\ell_i, bbox_i)$ (e.g., the latent codes are sampled from the standard normal distribution, $\mathcal{N}(0,1)$ under i.i.d. setting). Denote by $Z_{obj} = \{z_{obj_i}\}_{i=1}^m$ the set of object instance style latent codes.

Image synthesis from layout and style is the problem of learning a generation function which is capable of synthesizing an image defined on λ for a given input (L, z_{img}, Z_{obj}),

$$I = G(L, z_{img}, Z_{obj}; \Theta_G) \qquad (1)$$

where Θ_G represents the parameters of the generation function. Ideally, $G(\cdot)$ is expected to capture the underlying conditional data distribution $p(I|L, z_{img}, Z_{obj})$ in the high-dimensional space.

Reconfigurability of $G(\cdot)$. We are interested in three aspects in this paper:

- *Image style reconfiguration:* If we fix the layout L, is $G(\cdot)$ capable of generating images with different styles for different (z_{img}, Z_{obj})?

- *Object style reconfiguration:* If we fix the layout L, the image style z_{img} and object styles $Z_{obj} \setminus z_{obj_i}$, is $G(\cdot)$ capable of generating consistent images with different styles for the object $(\ell_i, bbox_i)$ using different z_{obj_i}?

- *Layout reconfiguration:* Given a (L, z_{img}, Z_{obj}), is $G(\cdot)$ capable of generating consistent images for different $(L^+, z_{img}, Z_{obj}^+)$ where we can add a new object to L^+ or just change the bounding box location of an existing object? When a new object is added, we also sample a new z_{obj} to add in Z_{obj}^+.

It is a big challenge to address the three aspects by learning a single generation function. It may be even difficult for well-trained artistic people to do so at scale (e.g., handling the 171 categories in the COCO-Stuff dataset). Due to the complexity that the generation function (Eqn. 1) needs to handle, it is parameterized (often over-parameterized) by powerful deep neural networks (DNNs). It is also well-known that training the DNN-based generation function individually is a extremely difficult task. Generative adversarial networks (GANs) [6] are entailed which are formulated under two-player minmax game settings.

3.2. The LostGAN

As Figure 2 shows, our LostGAN follows the traditional GAN pipeline with the following modifications.

3.2.1 The Generator

Figure 3 (a) shows the generator which utilizes the ResNet [8] architecture as backbone. Consider generating

64×64 images, the generator consists of 4 residual building blocks (ResBlocks). The image style latent code z_{img} is a d_{noise}-dim vector ($d_{noise} = 128$ in our experiments) whose elements are sampled from standard normal distribution under i.i.d. setting. Through a linear fully connected (FC) layer, z_{img} is projected to a $4 \times 4 \times (16 \times ch)$ dimensional vector which is then reshaped to $(4, 4, 16 \times ch)$ (representing height, width and channels) where ch is a hyperparameter to control model complexity (e.g., $ch = 64$ for generating 64×64 images). Then, each of the four ResBlocks upsamples its input with ratio 2 and bilinear interpolation. In the meanwhile, the feature channel will be decreased by ratio 2. For generating 128×128 images, we use 5 ResBlocks with $ch = 64$ and the same $d_{noise} = 128$ for z_{img}.

3.2.2 The ISLA-Norm

Figure 3 (b) shows the detail of ResBlock and the proposed ISLA-Norm. The ResBlock uses the basic block design as adopted in the projection-based cGAN [24] and Big-GAN [1]. Our ISLA-Norm first computes the mean and variance as done in BatchNorm [14], and then learns object instance-specific layout-aware affine transformation for each sample in a batch similar in spirit to the AdaIN used by the StyleGAN [18]. So, the feature normalization is computed in a batch manner, and the affine transformation is recalibrated in a sample-specific manner.

Denote by x the input 4D feature map of ISLA-Norm, and x_{nhwc} the feature response at position (n, h, w, c) (using the convention order of axes for batch, spatial height and width axis, and channel). We have $n \in [0, N-1]$, $h \in [0, H-1]$, $w \in [0, W-1]$ and $c \in [0, C-1]$ where H, W, C depend on the stage of a ResBlock.

In training, ISLA-Norm first normalizes x_{nhwc} by,

$$\hat{x}_{nhwc} = \frac{x_{nhwc} - \mu_c}{\sigma_c}, \qquad (2)$$

where the channel-wise batch mean $\mu_c = \frac{1}{N \cdot H \cdot W} \sum_{n,h,w} x_{nhwc}$ and standard deviation (std) $\sigma_c = \sqrt{\frac{1}{N \cdot H \cdot W} \sum_{n,h,w} (x_{nhwc} - \mu_c)^2 + \epsilon}$ (ϵ is a small positive constant for numeric stability). In standard Batch-Norm [14], for the affine transformation, a channel-wise γ_c and β_c will be learned and shared with all spatial locations and all samples in a batch. our ISLA-Norm will learn object instance-specific and layout-aware affine transformation parameters, γ_{nhwc} and β_{nhwc}, and then recalibrate the normalized feature responses by,

$$\tilde{x}_{nhwc} = \gamma_{nhwc} \cdot \hat{x}_{nhwc} + \beta_{nhwc}. \qquad (3)$$

Computing γ_{nhwc} and β_{nhwc}. Without loss of generality, we show how to compute the gamma and beta parameters for one sample, i.e., γ_{hwc} and β_{hwc}. As shown in Figure 3 (b), we have the following four steps.

i) Label Embedding. We use one-hot label vector for the m object instances and then we obtain the $m \times d_\ell$ one-hot label matrix (e.g., $d_\ell = 171$ in COCO-Stuff). For label embedding, we use a learnable $d_\ell \times d_e$ embedding matrix to obtain the vectorized representation for labels, resulting in the $m \times d_e$ label-to-vector matrix, where d_e represents the embedding dimension (e.g., $d_e = 128$ in our experiments). We also have the object style latent codes Z_{obj} which is a $m \times d_{noise}$ noise matrix (e.g., $d_{noise} = 128$ the same as z_{img}). We then concatenate the label-to-vector matrix and the noise matrix as the final $m \times (d_e + d_{noise})$ embedding matrix. So, the object instance style will depends on both the label embedding (semantics) and i.i.d. latent code (accounting for style variations).

ii) Object instance-specific projection. With the final embedding matrix, we compute object instance-specific channel-wise γ and β via linear projection with a learnable $(d_e + d_{noise}) \times 2C$ projection matrix where C is the number of channels.

iii) Mask prediction. The $s \times s$ mask for each object instance (e.g., $s = 16$ in our experiments) is predicted by a sub-network consisting of several up-sample convolution followed by sigmoid transformation. So, our predicted masks are not binary. Then, we resize the predicted masks to the sizes of corresponding bounding boxes.

iv) ISLA γ and β computation. We unsqueeze the object instance-specific channel-wise γ and β to their corresponding bounding boxes with the predicted mask weights multiplied. Then, we add them together with averaged sum used for overlapping regions.

3.2.3 The Discriminator

As shown in Figure 2, our discriminator consists of three components: the shared ResNet backbone, the image head classifier and the object head classifier.

The ResNet backbone has several ResBlocks (4 for 64×64 and 5 for 128×128) as in [24, 1]. The image head classifier consists of a ResBlock, a global average pooling layer and a fully-connected (FC) layer with one output unit, while object head classifier consists of ROI Align [7], a global average pooling layer and a FC layer with one output unit.

Following the projection-based cGANs [24] and the practice in BigGANs [1], we learn a separate label embedding for computing object adversarial hinge loss.

Denote by $D(\cdot; \Theta_D)$ the discriminator with parameters Θ_D. Given an image I (real or synthesized) and a layout L, the discriminator computes the prediction score for image and the average score for cropped objects, and we have,

$$(s_{img}, s_{obj}) = D(I, L; \Theta_D) \qquad (4)$$

3.2.4 The Loss Functions

To train (Θ_G, Θ_D) in our LostGAN, we utilize the hinge version [32, 22] of the standard adversarial loss [6],

$$l_t(I, L) = \begin{cases} \min(0, -1 + s_t); & \text{if } I \text{ is real} \\ \min(0, -1 - s_t); & \text{if } I \text{ is fake} \end{cases} \qquad (5)$$

where $t \in \{img, obj\}$. Let $l(I, L) = l_{img}(I, L) + \lambda \cdot l_{obj}(I, L)$ with λ the trade-off parameter for controlling the quality between synthesized images and objects ($\lambda = 1$ in our experiments). We have the expected losses for the discriminator and the generator,

$$\mathcal{L}(\Theta_D | \Theta_G) = - \mathop{\mathbb{E}}_{(I,L) \sim p(I,L)} [l(I, L)]$$
$$\mathcal{L}(\Theta_G | \Theta_D) = - \mathop{\mathbb{E}}_{(I,L) \sim p_{fake}(I,L)} [D(I, L; \Theta_D)] \qquad (6)$$

where $p(I, L)$ represents all the real and fake (by the current generator) data and $p_{fake}(I, L)$ represents the fake data.

4. Experiments

We test our LostGAN in the COCO-Stuff dataset [2] and the Visual Genome (VG) dataset [20]. We evaluate it for generating images at two resolutions 64×64 and 128×128. In comparison, the state-of-the-art methods include the very recent Layout2Im method [38], the scene graph to image (sg2im) method [16] and the pix2pix method [15].

4.1. Datasets

The **COCO-Stuff** 2017 [2] augments the COCO dataset with pixel-level stuff annotations. The annotation contains 80 *thing* classes (person, car, *etc.*) and 91 *stuff* classes (sky, road, *etc.*) Following settings of [16], objects covering less than 2% of the image are ignored, and we use images with 3 to 8 objects. The **Visual Genome** dataset [20]. Following settings of [16] to removing small and infrequent objects, we have 62,565 training, 5,506 val and 5,088 testing images with 3 to 30 objects from 178 categories in each image.

4.2. Evaluation Metrics

We evaluate quality and visual appearance of generated images by Inception Score (higher is better) [30] and Frèchet Inception Distance (FID, lower is better) [10], which use pretrained Inception [31] network to encourage recognizable objects within images and diversity across images. Diversity score computes perceptual similarity between two images (higher is better). We adopt LPIPS metric [37] to compute perceptual similarity in feature space between two images generated from same layout as diversity score. We also evaluate our model by recently proposed Classification Accuracy Score (CAS) [28].

4.3. Quantitative results

Table 1, 2 summarizes comparisons between our model and state-of-the-art models with respect to inception score,
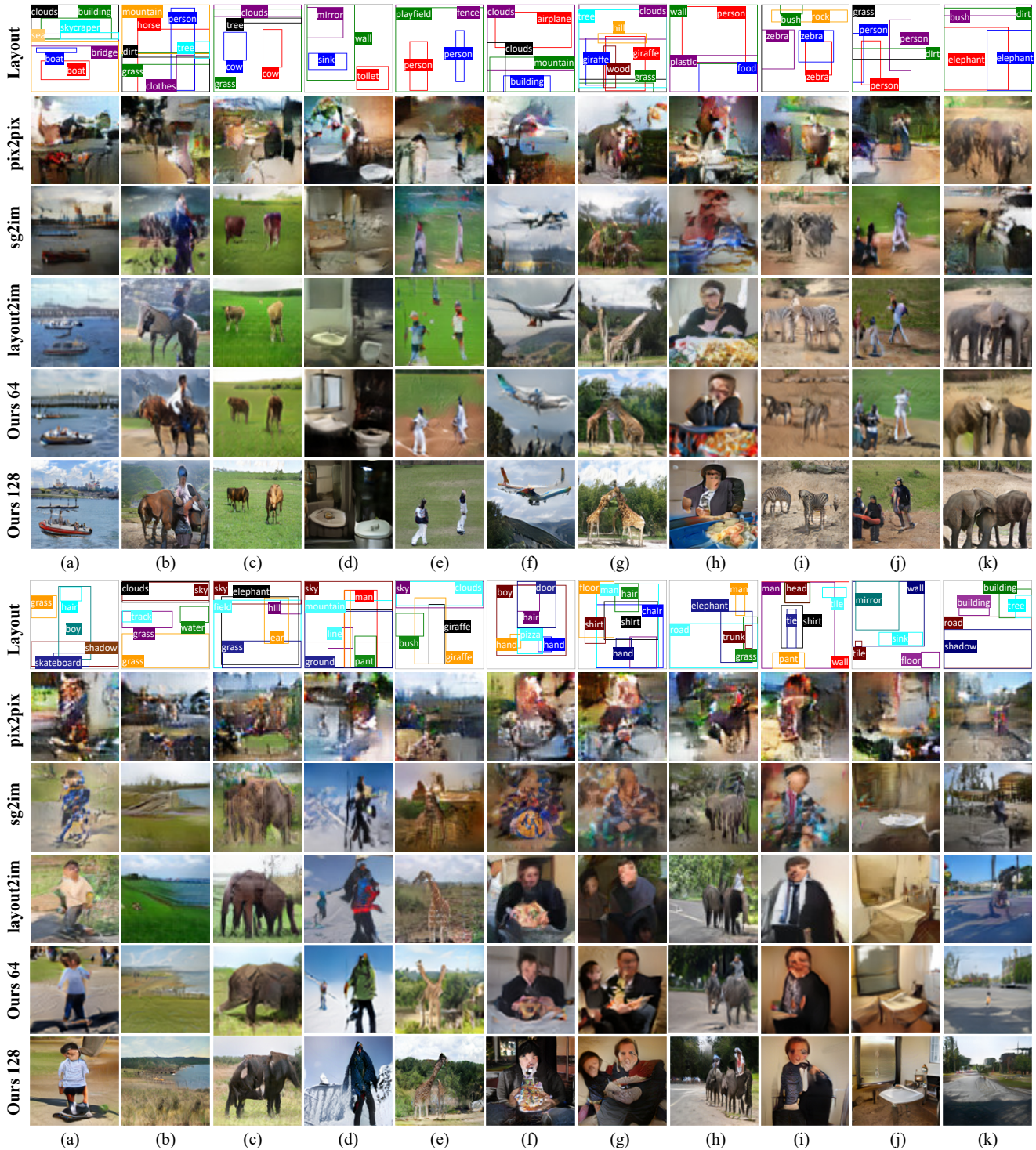
Figure 4. Generated samples from given layouts on COCO-Stuff (top) and Visual Genome (bottom). Images generated by pix2pix, sg2im, and layout2im are at 64×64 resolution.

FID, diversity score and classification accuracy. Our Lost-GAN outperforms the most recent Layout2Im [38] in terms of both Inception score and Diversity score. For 64×64 images, the improvement of Inception score, FID and classi-

fication accuracy indicates higher visual quality of image generated by our model. Diversity score is improved significantly which shows that our LostGAN can generate images with various appearance for a given layout. We also

Methods	Inception Score		FID		Diversity Score	
	COCO	VG	COCO	VG		
Real Images (64×64)	16.3 ± 0.4	13.9 ± 0.5	-	-	-	-
Real Images (128×128)	22.3 ± 0.5	20.5 ± 1.5	-	-	-	-
pix2pix	3.5 ± 0.1	2.7 ± 0.02	121.97	142.86	0	0
sg2im(GT Layout)	7.3 ± 0.1	6.3 ± 0.2	67.96	74.61	0.02 ± 0.01	0.15 ± 0.12
Layout2Im	9.1 ± 0.1	8.1 ± 0.1	38.14	40.07	0.15 ± 0.06	0.17 ± 0.09
Ours 64×64	**9.8 ± 0.2**	**8.7 ± 0.4**	**34.31**	**34.75**	**0.35 ± 0.09**	**0.34 ± 0.10**
Ours 128×128	**13.8 ± 0.4**	**11.1 ± 0.6**	29.65	29.36	0.40 ± 0.09	0.43 ± 0.09

Table 1. Quantitative comparisons using Inception Score (higher is better), FID (lower is better) and Diversity Score (higher is better) evaluation on COCO-Stuff and VG dataset. Images for pix2pix [15], sg2im [16] and Layout2Im [38] are at 64×64 resolution.
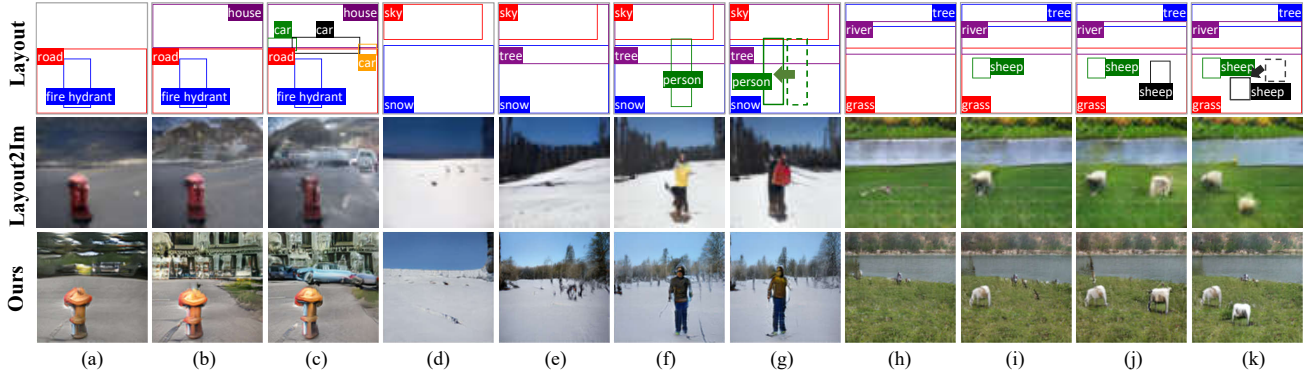

Figure 5. Generation results by adding new objects or change spatial position of objects.
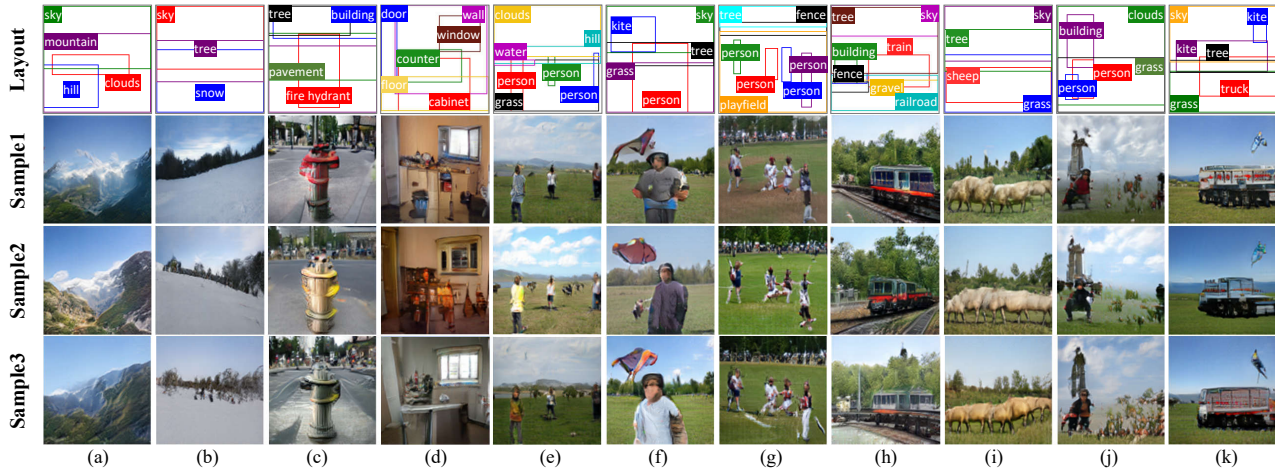

Figure 6. Multiple samples generated from same layout. Synthesized images have various visual appearance while preserving objects at desired location.

Figure 7. Linear interpolation of instance style. Top row indicates interpolation of style in sky, bottom row shows style morphing of grass.

conduct experiments at the resolution of 128×128, and our LostGAN obtains consistently better results.
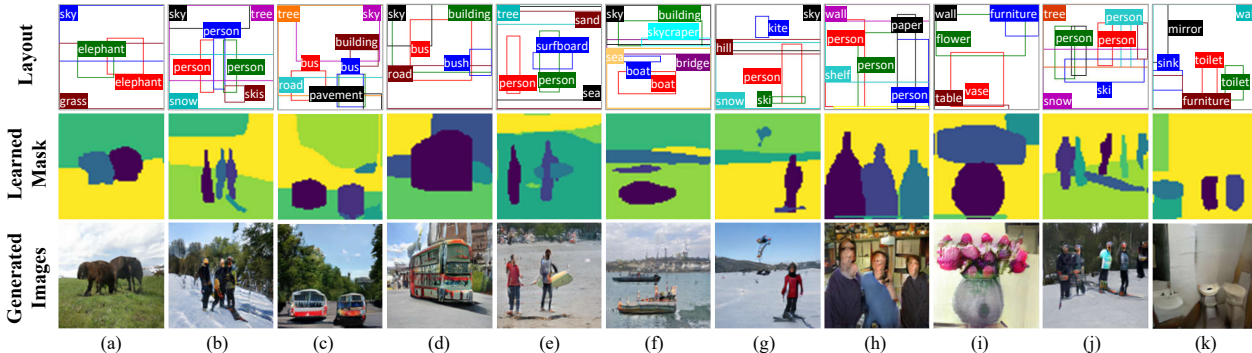
Figure 8. Synthesized images and learned masks for given layouts. Our proposed model learns masks from given layout in a weakly-supervised manner as ground truth mask for each object is not utilized during training.

Methods	Classification Accuracy	
	COCO	VG
Layout2im	27.32	23.25
Ours 64x64	28.81	27.50
Ours 128x128	28.70	25.89
Real Images	51.04	48.07

Table 2. Classification Accuracy Comparisons. We train resnet-101 on cropped objects from generated images (generate five samples for each layout) and evaluate on objects from real images.

4.4. Qualitative results

Figure 4 shows results of different models generating images from the same layout on both COCO-Stuff and VG. The input layouts are quite complex. Our LostGAN can generate visually more appealing images with more recognizable objects that are consistent with input layouts at resolution 64×64, and is further capable of synthesizing images at 128 × 128 resolution with better image quality.

We also conduct some ablation studies on the three aspects of reconfigurability and mask prediction.

Layout reconfiguration is demonstrated by adding object to or moving a bounding box in a layout (Figure 5). Our LostGAN shows better layout reconfigurability than the Layout2Im [38]. When adding extra objects or moving bounding box of one instance, our model can generate reasonable objects at desired position while keeping existing objects unchanged as we keep the input style of existing objects fixed. When moving bounding box of one object, style of generated object in new position can also be kept consistent, like (f) and (g), the person is moved while keep style feature like pose and color of clothes unaffected.

Image style reconfiguration To assess diversity of generation, multiple images are sampled from our LostGAN for each input layout (Figure 6). Our model can synthesize images with different visual appearance for a given layout while preserving objects at desired location.

Object instance style reconfiguration Our LostGAN is also capable of controlling styles at object instance level. Figure 7 shows results of gradually morphing styles of one

instance in different images. Top row shows how the style of sky gradually turns from blue to dusk while keeping styles of other objects unaltered. Bottom row displays how the style of grass transforms from green to withered.

Weakly-supervised mask prediction Figure 8 shows generated semantic label map when synthesizing images from given layouts. For pixels where bounding boxes of different objects overlap, their semantic labels are assigned by objects with the highest predicted mask weight. Unlike [12, 21] where ground truth masks is adopted to guide learning of shape generator, our model can learn semantic masks in a weakly-supervised manner. Even for objects with overlapped bounding box, like person and surfboard in (f), synthesized images and learned masks are consistent and semantically reasonable.

5. Conclusion

This paper presents a layout- and style-based architecture for generative adversarial networks (LostGANs) that can be trained end-to-end to generate images from reconfigurable layout and style. The proposed LostGAN can learn fine-grained mask maps in a weakly-supervised manner to bridge the gap between layouts and images, and proposes the object instance-specific layout-aware feature normalization (ISLA-Norm) in the generator to realize multi-object style generation. State-of-the-art performance is obtained on COCO-Stuff and VG dataset. Qualitative results demonstrate the proposed model is capable of generating scene images with reconfigurable layout and instance-level style control.

Acknowledgement

References

[1] Andrew Brock, Jeff Donahue, and Karen Simonyan. Large scale gan training for high fidelity natural image synthesis. *arXiv preprint arXiv:1809.11096*, 2018. 1, 2, 3, 4, 5

[2] Holger Caesar, Jasper Uijlings, and Vittorio Ferrari. Coco-stuff: Thing and stuff classes in context. In *Proceedings of the IEEE Conference on Computer Vision and Pattern Recognition*, pages 1209–1218, 2018. 3, 5

[3] Harm De Vries, Florian Strub, Jérémie Mary, Hugo Larochelle, Olivier Pietquin, and Aaron C Courville. Modulating early visual processing by language. In *Advances in Neural Information Processing Systems*, pages 6594–6604, 2017. 3

[4] Vincent Dumoulin, Ishmael Belghazi, Ben Poole, Olivier Mastropietro, Alex Lamb, Martin Arjovsky, and Aaron Courville. Adversarially learned inference. *arXiv preprint arXiv:1606.00704*, 2016. 3

[5] Vincent Dumoulin, Jonathon Shlens, and Manjunath Kudlur. A learned representation for artistic style. *Proc. of ICLR*, 2, 2017. 3

[6] Ian Goodfellow, Jean Pouget-Abadie, Mehdi Mirza, Bing Xu, David Warde-Farley, Sherjil Ozair, Aaron Courville, and Yoshua Bengio. Generative adversarial nets. In *Advances in neural information processing systems*, pages 2672–2680, 2014. 1, 3, 4, 5

[7] Kaiming He, Georgia Gkioxari, Piotr Dollár, and Ross Girshick. Mask r-cnn. In *Proceedings of the IEEE international conference on computer vision*, pages 2961–2969, 2017. 5

[8] Kaiming He, Xiangyu Zhang, Shaoqing Ren, and Jian Sun. Deep residual learning for image recognition. In *Proceedings of the IEEE conference on computer vision and pattern recognition*, pages 770–778, 2016. 2, 4

[9] Martin Heusel, Hubert Ramsauer, Thomas Unterthiner, Bernhard Nessler, and Sepp Hochreiter. GANs trained by a two time-scale update rule converge to a local nash equilibrium. In *NIPS*, 2017. 3

[10] Martin Heusel, Hubert Ramsauer, Thomas Unterthiner, Bernhard Nessler, and Sepp Hochreiter. Gans trained by a two time-scale update rule converge to a local nash equilibrium. In *Advances in Neural Information Processing Systems*, pages 6626–6637, 2017. 5

[11] Tobias Hinz, Stefan Heinrich, and Stefan Wermter. Generating multiple objects at spatially distinct locations. *arXiv preprint arXiv:1901.00686*, 2019. 3

[12] Seunghoon Hong, Dingdong Yang, Jongwook Choi, and Honglak Lee. Inferring semantic layout for hierarchical text-to-image synthesis. In *Proceedings of the IEEE Conference on Computer Vision and Pattern Recognition*, pages 7986–7994, 2018. 2, 3, 8

[13] Xun Huang, Ming-Yu Liu, Serge Belongie, and Jan Kautz. Multimodal unsupervised image-to-image translation. In *Proceedings of the European Conference on Computer Vision (ECCV)*, pages 172–189, 2018. 3

[14] Sergey Ioffe and Christian Szegedy. Batch normalization: Accelerating deep network training by reducing internal covariate shift. *arXiv preprint arXiv:1502.03167*, 2015. 3, 4

[15] Phillip Isola, Jun-Yan Zhu, Tinghui Zhou, and Alexei A Efros. Image-to-image translation with conditional adversarial networks. In *Proceedings of the IEEE conference on computer vision and pattern recognition*, pages 1125–1134, 2017. 2, 3, 5, 7

[16] Justin Johnson, Agrim Gupta, and Li Fei-Fei. Image generation from scene graphs. In *Proceedings of the IEEE Conference on Computer Vision and Pattern Recognition*, pages 1219–1228, 2018. 2, 3, 5, 7

[17] Tero Karras, Timo Aila, Samuli Laine, and Jaakko Lehtinen. Progressive growing of gans for improved quality, stability, and variation. *arXiv preprint arXiv:1710.10196*, 2017. 1

[18] Tero Karras, Samuli Laine, and Timo Aila. A style-based generator architecture for generative adversarial networks. *arXiv preprint arXiv:1812.04948*, 2018. 1, 2, 3, 4

[19] Taeksoo Kim, Moonsu Cha, Hyunsoo Kim, Jung Kwon Lee, and Jiwon Kim. Learning to discover cross-domain relations with generative adversarial networks. In *Proceedings of the 34th International Conference on Machine Learning-Volume 70*, pages 1857–1865. JMLR. org, 2017. 3

[20] Ranjay Krishna, Yuke Zhu, Oliver Groth, Justin Johnson, Kenji Hata, Joshua Kravitz, Stephanie Chen, Yannis Kalantidis, Li-Jia Li, David A Shamma, et al. Visual genome: Connecting language and vision using crowdsourced dense image annotations. *International Journal of Computer Vision*, 123(1):32–73, 2017. 3, 5

[21] Wenbo Li, Pengchuan Zhang, Lei Zhang, Qiuyuan Huang, Xiaodong He, Siwei Lyu, and Jianfeng Gao. Object-driven text-to-image synthesis via adversarial training. *arXiv preprint arXiv:1902.10740*, 2019. 3, 8

[22] Jae Hyun Lim and Jong Chul Ye. Geometric gan. *arXiv preprint arXiv:1705.02894*, 2017. 3, 5

[23] Takeru Miyato, Toshiki Kataoka, Masanori Koyama, and Yuichi Yoshida. Spectral normalization for generative adversarial networks. *arXiv preprint arXiv:1802.05957*, 2018. 1, 3

[24] Takeru Miyato and Masanori Koyama. cgans with projection discriminator. *arXiv preprint arXiv:1802.05637*, 2018. 1, 2, 3, 4, 5

[25] Augustus Odena, Christopher Olah, and Jonathon Shlens. Conditional image synthesis with auxiliary classifier gans. In *Proceedings of the 34th International Conference on Machine Learning-Volume 70*, pages 2642–2651. JMLR. org, 2017. 3

[26] Taesung Park, Ming-Yu Liu, Ting-Chun Wang, and Jun-Yan Zhu. Semantic image synthesis with spatially-adaptive normalization. In *Proceedings of the IEEE Conference on Computer Vision and Pattern Recognition*, pages 2337–2346, 2019. 3

[27] Alec Radford, Luke Metz, and Soumith Chintala. Unsupervised representation learning with deep convolutional generative adversarial networks. *arXiv preprint arXiv:1511.06434*, 2015. 1

[28] Suman Ravuri and Oriol Vinyals. Classification accuracy score for conditional generative models. *arXiv preprint arXiv:1905.10887*, 2019. 3, 5

[29] Scott Reed, Zeynep Akata, Xinchen Yan, Lajanugen Logeswaran, Bernt Schiele, and Honglak Lee. Generative adversarial text to image synthesis. *arXiv preprint arXiv:1605.05396*, 2016. 3

[30] Tim Salimans, Ian Goodfellow, Wojciech Zaremba, Vicki Cheung, Alec Radford, and Xi Chen. Improved techniques for training gans. In *Advances in neural information processing systems*, pages 2234–2242, 2016. 3, 5

[31] Christian Szegedy, Wei Liu, Yangqing Jia, Pierre Sermanet, Scott Reed, Dragomir Anguelov, Dumitru Erhan, Vincent Vanhoucke, and Andrew Rabinovich. Going deeper with convolutions. In *Proceedings of the IEEE conference on computer vision and pattern recognition*, pages 1–9, 2015. 5

[32] Dustin Tran, Rajesh Ranganath, and David M Blei. Deep and hierarchical implicit models. *arXiv preprint arXiv:1702.08896*, 7, 2017. 3, 5

[33] Ting-Chun Wang, Ming-Yu Liu, Jun-Yan Zhu, Andrew Tao, Jan Kautz, and Bryan Catanzaro. High-resolution image synthesis and semantic manipulation with conditional gans. In *Proceedings of the IEEE Conference on Computer Vision and Pattern Recognition*, pages 8798–8807, 2018. 2, 3

[34] Tao Xu, Pengchuan Zhang, Qiuyuan Huang, Han Zhang, Zhe Gan, Xiaolei Huang, and Xiaodong He. Attngan: Fine-grained text to image generation with attentional generative adversarial networks. In *Proceedings of the IEEE Conference on Computer Vision and Pattern Recognition*, pages 1316–1324, 2018. 2

[35] Han Zhang, Ian Goodfellow, Dimitris Metaxas, and Augustus Odena. Self-attention generative adversarial networks. *arXiv preprint arXiv:1805.08318*, 2018. 1, 3

[36] Han Zhang, Tao Xu, Hongsheng Li, Shaoting Zhang, Xiaogang Wang, Xiaolei Huang, and Dimitris N Metaxas. Stackgan: Text to photo-realistic image synthesis with stacked generative adversarial networks. In *Proceedings of the IEEE International Conference on Computer Vision*, pages 5907–5915, 2017. 2, 3

[37] Richard Zhang, Phillip Isola, Alexei A Efros, Eli Shechtman, and Oliver Wang. The unreasonable effectiveness of deep features as a perceptual metric. In *Proceedings of the IEEE Conference on Computer Vision and Pattern Recognition*, pages 586–595, 2018. 3, 5

[38] Bo Zhao, Lili Meng, Weidong Yin, and Leonid Sigal. Image generation from layout. *arXiv preprint arXiv:1811.11389*, 2018. 2, 3, 5, 6, 7, 8

[39] Jun-Yan Zhu, Taesung Park, Phillip Isola, and Alexei A Efros. Unpaired image-to-image translation using cycle-consistent adversarial networks. In *Proceedings of the IEEE International Conference on Computer Vision*, pages 2223–2232, 2017. 3